Carbohydrate Polymers 204 (2019) 131–141

Contents lists available at ScienceDirect

Carbohydrate Polymers

journal homepage: www.elsevier.com/locate/carbpol

Controlling the degradation of an oxidized dextran-based hydrogel independent of the mechanical properties

Punnida Nonsuwan[a,b], Akimasa Matsugami[c], Fumiaki Hayashi[c], Suong-Hyu Hyon[d], Kazuaki Matsumura[a,*]

[a] School of Materials Science, Japan Advanced Institute of Science and Technology, 1-1 Asahidai, Nomi, Ishikawa 923-1292, Japan
[b] Department of Chemistry, Faculty of Science, Chulalongkorn University, 254 Phayathai Road, Pathumwan, Bangkok 10330, Thailand
[c] Advanced NMR Application and Platform Team, NMR Research and Collaboration Group, NMR Science and Development Division, RIKEN SPring-8 Center, 1-7-22 Suehiro-cho, Tsurumi-ku, Yokohama, Kanagawa 230-0045, Japan
[d] Joint Faculty of Veterinary Medicine, Kagoshima University, 1-21-24, Korimoto, Kagoshima 890-8580, Japan

ARTICLE INFO

Keywords:
Hydrogel
Biodegradation
Aldehyde dextran
Biomaterials
Drug delivery

ABSTRACT

The objective of this study is to control and elucidate the mechanism of molecular degradation in a polysaccharide hydrogel. Glycidyl methacrylate (GMA) immobilized dextran (Dex-GMA) was oxidized by periodate to introduce aldehyde groups (oxidized Dex-GMA). The hydrogel was formed by the addition of dithiothreitol to the oxidized Dex-GMA solution through thiol Michael addition with the preservation of the aldehyde group for degradation points. It was experimentally determined that the degradation of this hydrogel can be controlled by the addition of amino groups and the speed of degradation can be controlled independently of mechanical properties because crosslinking and degradation points are different. In addition, the molecular mechanism of the crosslinking between the thiol and aldehyde groups was found to control the degradation of dextran derivatives. It is expected that these results will be beneficial in the design of polymer materials in which the speed of degradation can be precisely controlled. In addition, the cytotoxicity of oxidized Dex-GMA was approximately 3000 times lower than that of glutaraldehyde. The low cytotoxicity of the aldehyde in oxidized Dex-GMA was the likely reason for the harmless functionalized polysaccharide material. Possible future clinical applications include cell scaffolds in regenerative medicine and carriers for drug delivery systems.

1. Introduction

Hydrogels are crosslinked polymer networks with a large number of hydrophilic domains. They can expand in numerous solvents and aqueous environments without dissolving owing to the chemical or physical bonds formed between polymer chains (Bhattarai, Gunn, & Zhang, 2010; Hoare & Kohane, 2008). Natural polymers, specifically polysaccharides, are frequently used for hydrogel preparation because of their biocompatibility and chemical structure; this facilitates the development of desirable functionalized materials (Maia, Ferreira, Carvalho, Ramos, & Gil, 2005). Until now, low-toxicity, biocompatible, and degradable hydrogels have been designed using polysaccharides and functionalized polysaccharides for biomedical applications such as tissue engineering scaffolds, wound dressings, and controlled drug delivery systems (Chen et al., 2017; Ferreira et al., 2007; Jukes et al., 2010; Mehvar, 2000; Möller, Weisser, Bischoff, & Schnabelrauch, 2007; Van Tomme & Hennink, 2007; Zhao et al., 2015). For example, alginate and its derivative hydrogels are compatible with a variety of techniques for controlling gelling and possess desirable physical and chemical properties that can be used to facilitate cell adhesion and control the speed of degradation, all of which can be combined to promote cell transplantation (Augst, Kong, & Mooney, 2006). The periodate oxidation of alginate, which can be crosslinked with multivalent cations (Ca^{2+}) to produce hydrogels, was observed to degrade in vitro in a phosphate buffer saline solution (PBS) (pH 7.4, 37 °C) within nine days (Bouhadir et al., 2001). These hydrogels can potentially be used in cartilage-like tissue formation. In addition, self-healing polysaccharide hydrogels were developed (Zhao et al., 2015). Hydrogel networks are attributed to two sensitive crosslinked bonds, i.e., imine bonds and acylhydrazone bonds, which impart the self-healing capability of hydrogels. The same group explored the integration of carboxymethyl cellulose-based hydrogels with photoluminescent performance to provide the dual function of self-healing and photoluminescence under ultraviolet light (Chen et al., 2017). Such a hydrogel can be developed

* Corresponding author.
E-mail address: mkazuaki@jaist.ac.jp (K. Matsumura).

https://doi.org/10.1016/j.carbpol.2018.09.081
Received 10 July 2018; Received in revised form 12 September 2018; Accepted 28 September 2018
Available online 03 October 2018

as a sealant for vessels and stomach mucosa perforation. The position of an adhesive hydrogel can be easily detected using a photoluminescent emitter; this provides high potential for application in the tissue engineering field. Focusing on hydrogel drug delivery systems, an active therapeutic agent was integrated with a polymeric network structure that could control its release rate by allowing a hydrogel to safely degrade in the body when it was no longer required (Jogani, Jinturkar, Vyas, & Misra, 2008). Biodegradable polysaccharides, such as chitosan, alginate, xanthan gum, and dextran, have been widely researched for potential applications in drug carriers (Debele, Mekuria, & Tsai, 2016; Liu, Jiao, Wang, Zhou, & Zhang, 2008; Morris, Kok, Harding, & Adams, 2010; Togo et al., 2013). Among these, dextran has received significant attention.

Dextran is a bacterial polysaccharide that is broadly applicable in the biomedical field owing to its biocompatibility (Cadee et al., 2000; Ferreira et al., 2004), low toxicity (Hyon, Nakajima, Sugai, & Matsumura, 2014), high natural abundance, and ability to degrade via enzymes in various parts of the human body such as the spleen, liver, and colon. In addition, it is available in a wide range of molecular weights (Khalikova, Susi, & Korpela, 2005; Mehvar, 2000) Furthermore, dextran contains a large number of hydroxyl groups, which provide it with high hydrophilicity and enable it to be used in chemical functionalization (Levesque & Shoichet, 2007; Maia et al., 2005; Massia & Stark, 2001; Mehvar, 2000). Hyon et al. (2014) prepared hydrogels via the reaction between the aldehyde groups in periodate oxidized dextran and the amino groups in poly-L-lysine. In this case, the hydrogels exhibited degradation in PBS. Degradation time could be controlled by the rate of aldehyde introduction and amine concentration. The mechanism of the degradation was reported as follows: The main chain of the oxidized dextran was degraded by the Maillard reaction, which was triggered by Schiff base formation between the aldehyde and amino groups. A two-dimensional (2D) nuclear magnetic resonance (NMR) scan revealed that the partial hemiacetal structures produced by the periodate oxidation reacted with the amino groups and underwent an Amadori rearrangement, which led to the scission of the glucose unit ring (Chimpibul et al., 2016) (Fig. S1). This study is based on this reaction, which is utilized to overcome the following drawback: In previous works, degradation speed depended on the number of chemical crosslink points during gelation because the crosslink points formed by the reaction between the aldehyde groups in the oxidized dextran and the amino groups in poly-L-lysine triggered the degradation of the hydrogel (Kirchhof et al., 2015; Togo et al., 2013). However, as the formation and degradation of this hydrogel occurred simultaneously after the Schiff base formation reaction between the aldehyde and amino groups, it was difficult to control the timing of the degradation. In addition, as the mechanical properties of the hydrogel were determined by the number of crosslinking points, degradation time also depended on mechanical properties, much like stiff hydrogels exhibit longer degradation times while soft hydrogels exhibit shorter degradation times. If degradation control that is independent of mechanical properties, such as hard/fast or soft/slow combinations, can be identified with respect to time and space, these hydrogels could prove to be valuable platform materials for the fabrication of biodegradable scaffolds and drug carriers.

In this study, glycidyl methacrylate (GMA) was immobilized into dextran (Dex-GMA) and oxidized by sodium periodate to introduce aldehyde groups, thereby creating oxidized Dex-GMA. Oxidized Dex-GMA was crosslinked with dithiothreitol (DTT) by a thiol Michael addition reaction to form a hydrogel with the remaining aldehyde groups. Then, a posteriori degradation was controlled by the addition of an amine source so that the degradation was independent of the mechanical properties of the hydrogels. It is considered that this novel strategy may open new avenues of approach to create tissue engineering and drug delivery system materials via unique chemical stimuli (amino group) responsive degradation control.

2. Experimental procedure

2.1. Materials

Dextran (molecular weight (Mw) = 70 kDa) was acquired from Meito Sangyo (Nagoya, Japan), GMA and DTT were purchased from TCI (Tokyo, Japan), and 4-Dimethylaminopyridine (DMAP) was obtained from Sigma Aldrich (St. Louis, MO, USA). Acetyl cysteine (Ac-Cys-OH) was obtained from Watanabe Chemical Ind., Ltd. (Hiroshima, Japan), and sodium periodate ($NaIO_4$), disodium hydrogen phosphate (Na_2HPO_4), sodium dihydrogen phosphate (NaH_2PO_4), glycine, and other chemicals were purchased from Nacalai Tesque, Inc. (Kyoto, Japan). All chemicals were used without purification.

2.2. Synthesis of oxidized Dex-GMA

Dex-GMA was synthesized by applying the method reported by Liu et al. (2015). 5 g of dextran was combined with 20 mL of dimethyl sulfoxide (DMSO), and the solution was stirred until dextran was completely dissolved. Then, the transparent solution was stirred for 30 min under nitrogen gas. Next, 0.8 g (6.5 mmol) of DMAP and 2.2 g (15.5 mmol) of GMA were added to the solution under nitrogen gas for 30 min. The solution was stirred at 50 °C for 12 h, followed by the addition of 6.5 mmol of hydrochloric acid (HCl) to the solution mixture to neutralize DMAP. The mixture was dialyzed against distilled water for one week using a dialysis membrane (MWCO = 3.5 kD). The resulting product was air dried for 48 h at 47 °C and vacuum dried for 48 h at 25 °C to obtain the Dex-GMA derivative as a pale yellow-brown flake product.

Oxidized Dex-GMA was synthesized by the oxidation of Dex-GMA with sodium periodate (Hyon et al., 2014). Here, 2.5 g of Dex-GMA was dissolved in 10 mL of distilled water, and various amounts of sodium periodate (0.375, 0.75, and 1.25 g) were dissolved in 5 mL water. The solutions of Dex-GMA and sodium periodate were mixed, and the reaction was allowed to continue at 50 °C for 1 h. The mixture was dialyzed against distilled water for 32 h using a dialysis membrane (MWCO = 3.5 kD). The resulting product was processed by air drying for 48 h at 47 °C and freeze drying for 48 h to obtain oxidized Dex-GMA. In addition, oxidized dextran without GMA was synthesized by following the same method, except that dextran was employed as the starting material.

2.3. Characterization of oxidized Dex-GMA

2.3.1. Characterization of oxidized Dex-GMA with nuclear magnetic resonance (NMR) spectroscopy

The synthesized products were characterized by ^{1}H NMR (600, 700, and 900 MHz equipped with a cryogenic probe, Bruker). Two-dimensional NMR techniques were used to analyze oxidized Dex-GMA, including ^{1}H–^{13}C heteronuclear single quantum correlation spectroscopy (HSQC), ^{1}H–^{13}C heteronuclear multiple-bond correlation spectroscopy (HMBC), total correlation spectroscopy (TOCSY), and double quantum filtered-correlation spectroscopy (DQF-COSY). The results of the ^{1}H NMR spectroscopy were used to investigate the degree of substitution (% DS) by comparing the ratio of the area under the proton peaks at 2.0 ppm (methyl protons in GMA) to the peak at 3.3–4.2 ppm (dextran sugar unit protons).

2.3.2. Determination of aldehyde content

The amount of aldehyde content in functionalized dextran was determined using the fluorometry method (Li, Sritharathikhun, & Motomizu, 2007). To prepare the mixture solution, 2.5 ml of 4.0 M ammonium acetate, 1.0 ml of 0.2 M acetoacetanilide (AAA), 1.0 ml of ethanol, and a series of standard glutaraldehyde solutions or samples were combined. Then, the mixtures were diluted to 5 mL with purified water and left for 10 min. The relative fluorescence intensities of the

reagent blank, standard glutaraldehyde, and sample solutions were measured at 470 nm with an excitation wavelength of 370 nm. The aldehyde content was determined from the standard calibration graph.

2.3.3. Gelation time measurement

Gels can form when oxidized Dex-GMA is crosslinked by DTT. The same volume of 10% (w/v) of oxidized Dex-GMA (23% DS of GMA and 24% degree of oxidation) and 1.00, 1.36, or 2.72% (w/v) of DTT in PBS, in which the molar ratio of C=C and thiol was equivalent at 1:0.74, 1:1, and 1:2, were mixed in a test tube. Gelation time was investigated through rheology analysis at a temperature of 37 °C. The molar ratio of the functional groups was varied by changing the concentration of DTT to determine gelling time.

2.3.4. Rheological characterization

Rheological properties were evaluated using a rheometer equipped with a 24.99 mm, 2.069° cone (Rheosol G5000, UBM Co., Ltd., Kyoto, Japan). 10% (w/v) of oxidized Dex-GMA (23% DS of GMA with varying degrees of oxidation) and 1 or 1.36% (w/v) of DTT in PBS with the same volume were mixed and placed in the gap between the lower plate and cone while temperature was maintained at 37 °C. The dynamic storage (G') and loss (G") moduli of the hydrogels were determined via a frequency dispersion mode from 0.01 to 10 Hz.

Crosslink density can be estimated from the plateau storage modulus, G', of a hydrogel according to the following equation:

$$G' = \nu kT$$

where k and T denote the Boltzmann constant ($1.38 \times 10^{-23}\ m^2\ kg\ s^{-2}\ K^{-1}$) and temperature (K), respectively. In this study, temperature was 310 K.

2.3.5. Determination of the rate of gel degradation

To quantitatively evaluate the degradation of the gel, 0.5 mL of a 10% (w/v) oxidized Dex-GMA (23% DS of GMA with varying degrees of oxidation) aqueous solution and 0.5 mL of 1.36 wt% DTT were mixed in a centrifuge tube (15 mL capacity). The mixture was incubated at 37 °C for 30 min in a water bath to allow for gelation. After the addition of 10 mL of PBS and an amino compound solution (1–10% (w/v) glycine solution), the tube was tightly sealed and incubated at 37 °C while being gently rotated. After the time interval had elapsed, the supernatant was removed and the remaining gel was rinsed with distilled water. Then, the remaining gel was freeze dried (48 h) and vacuum dried (50 °C for 24 h). The weight of the remaining hydrogel was recorded versus the incubation periods. Samples were obtained in triplicate (n = 3).

2.3.6. Determination of molecular weight (Mw) by gel permeation chromatography (GPC)

Oxidized dextran and oxidized Dex-GMA at 24% oxidation were dissolved in a phosphate buffer solution (pH 7.4, 0.1 M) to achieve the desired final concentration of 2% (w/v). A monothiol reagent (Ac-Cys-OH) was used instead of DTT so as to not form a hydrogel. The same volume of glycine (or Ac-Cys-OH) with a concentration of 0.6% and 5% (w/v) was added to the dextran derivative solution, which was then incubated at 37 °C. Glycine was used as an amine source, and Ac-Cys-OH was used as an SH source. Gel permeation chromatography (GPC) was performed using a differential refractive index detector, which offers comparatively uniform mass sensitivity (Shimadzu, Japan, BioSep-s2000 column, Phenomenex, Inc., CA, USA), to determine the molecular weight of the dextran derivatives at the desired time after the reaction. Here, PBS was used as the mobile phase (flow rate = 0.50 mL/min) and pullulan was used as the standard.

2.3.7. Determination of thiol content by Ellman's assay

To characterize the reaction of the aldehyde in oxidized Dex-GMA with DTT, oxidized dextran without GMA was used as the model to react with the mono-thiol reagent. Ellman's reagent, which is also known as 5,5′-Dithio-bis-(2-nitrobenzoic acid) or DTNB, was employed to evaluate the sulfhydryl group in the sample. A set of test tubes was prepared, each of which contained 2.5 mL of reaction buffer (0.1 M phosphate buffer, pH 8), 1 mM of ethylenediaminetetraacetic acid (EDTA), and 50 μL of Ellman's reagent solution (created by dissolving 4 mg of Ellman's reagent in 1 mL of reaction buffer). Then, standard cysteine (0–1.5 mM) or 250 μL of an unknown solution was added to a separate test tube. The solution was mixed and incubated at 25 °C for 15 min, and then, absorbance was measured at 412 nm. The concentration of the experimental sample was determined by comparison with the calibration graph of standard cysteine.

2.3.8. Kinetic analysis by NMR spectroscopy

The NMR data were recorded on a Bruker Avance III 600, 700, and 900 MHz spectrometer equipped with a cryogenic probe at 25 °C for use in the kinetic analysis of the reactions between oxidized dextran-GMA and Ac-Cys-OH or glycine. Two-dimensional NMR techniques, including ^{1}H–^{13}C HSQC, ^{1}H–^{13}C HMBC, TOCSY, and DQF-COSY, were used to analyze oxidized Dex-GMA. In the kinetic analysis experiments, Dex-GMA [10% (w/w)] oxidized with $NaIO_4$ [(30% (w/w)] and 6% (w/w) Ac-Cys-OH or glycine, both in a PBS/D_2O solution at a pH of 7, were mixed in a ratio of 1:1 in an ice bath to delay degradation. The final concentration was 5% oxidized Dex-GMA and 3% Ac-Cys-OH or glycine. As the peak was broadened owing to the high concentration of Ac-Cys-OH, the reaction between 5% oxidized Dex-GMA and 0.75% Ac-Cys-OH (low concentration Ac-Cys-OH) was monitored via NMR. Once the solution was mixed, it was immediately transferred to the NMR spectrometer, and the first ^{1}H NMR spectrum was recorded 12–17 min later. Subsequently, one-dimensional ^{1}H NMR spectra with presaturation were recorded every 5 min, and 24 scans were obtained with a recycle time of 12.5 s.

2.3.9. Determination of cytotoxicity

Cell viability was determined by measuring the ability of the cells to convert 3-(4,5-dimethyl thial-2-yl)-2, 5-diphenyltetrazalium bromide (MTT) to a purple formazan dye. L929 cells suspended in a 0.1 mL medium at a concentration of 1.0×10^4/mL were placed in 96-well culture plates. After incubation for 72 h at 37 °C, 0.1 mL of the medium containing different concentrations of Ox(24%)-GMA(23%)-Dex was added to the cells, followed by incubation for 48 h. To evaluate cell viability, 0.1 mL MTT solution (300 mg/mL in medium) was added to the cultured cells, which were further incubated for 4 h at 37 °C. After removing the remaining medium, 0.1 mL DMSO was added to each well to dissolve the precipitate. The resulting color intensity, which was proportional to the number of viable cells, was measured by a microplate reader (versa max, Molecular Devices Co., CA, USA) at 540 nm. The cytotoxicity of the test substances was expressed as the 50% inhibition concentration of growth (IC50), which was defined as the concentration in the culture at which cell activity was reduced to 50% of that of the untreated control cells.

3. Results and discussion

3.1. Characterization of oxidized Dex-GMA with NMR

The concept of this study is depicted in Fig. 1. Dex-GMA was synthesized in two steps, as shown in Fig. 1A. In the first step, dextran was modified by GMA in DMSO using the method described in literature (Liu et al., 2015). The reaction between GMA and dextran proceeded via the nucleophilic attack of a hydroxyl group of dextran on the methylene carbon of the epoxy group of GMA (Reis et al., 2009; Van Dijk-Wolthuis et al., 1995). Then, the dried Dex-GMA product was oxidized by $NaIO_4$ to introduce aldehyde groups via Malaprade oxidation (Hyon et al., 2014). The formation of a hydrogel was accomplished by adding DTT to react with C=C and SH via a thiol Michael addition reaction

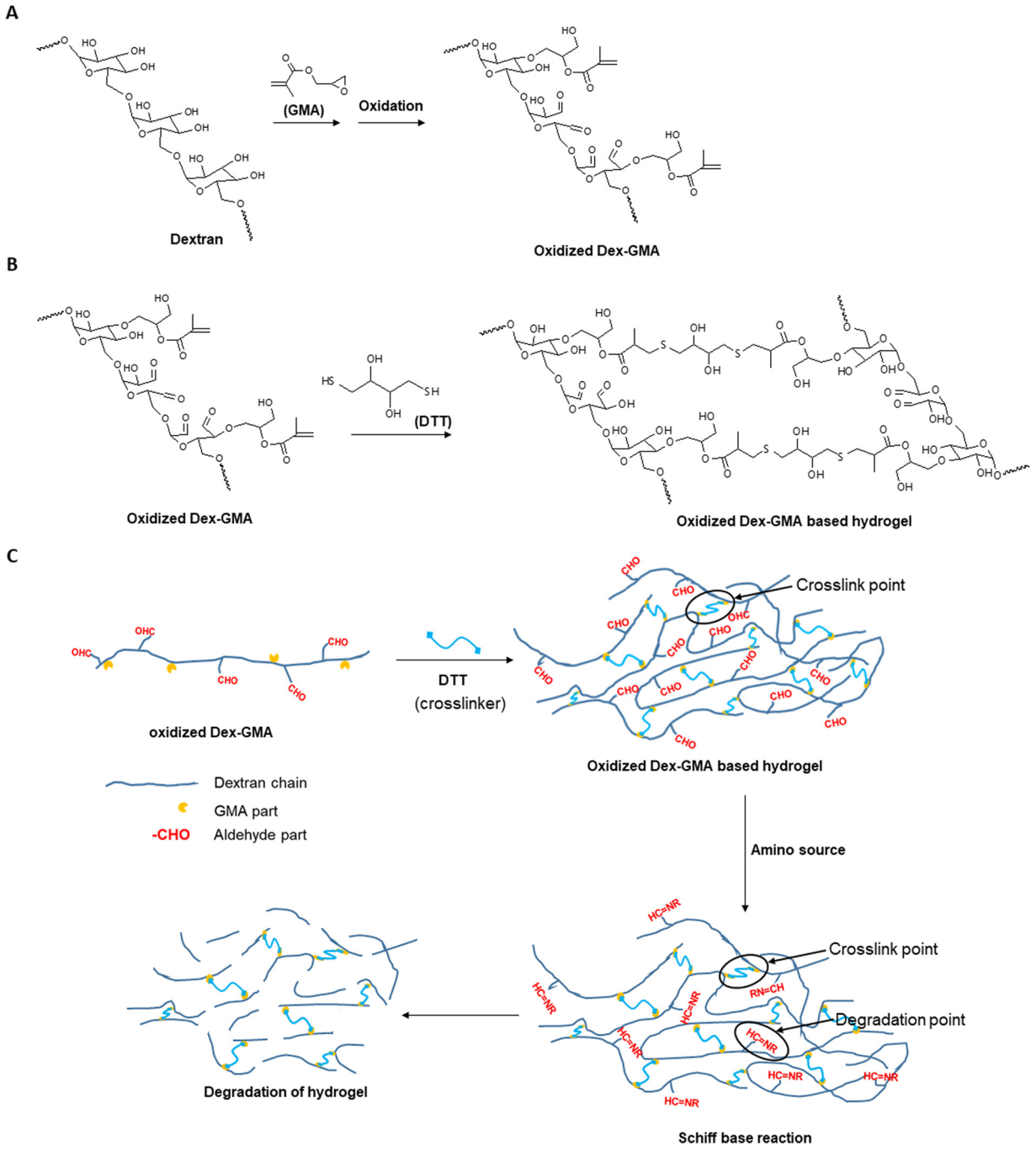

Fig. 1. Synthesis of an oxidized Dex-GMA based hydrogel. (A) Process used to synthesize oxidized Dex-GMA. (B) Proposed model of an oxidized Dex-GMA based hydrogel. (C) Schematic depiction of the formation of an oxidized Dex-GMA based hydrogel and its subsequent degradation by the addition of amino groups.

with the remaining aldehyde groups (Fig. 1B). In addition, an amine source was added to the hydrogel to react with the aldehyde to form a Schiff base and initiate the degradation of the hydrogels, which resulted in a Maillard reaction (Fig. 1C).

The assignments of oxidized Dex-GMA were conducted with ^{1}H–^{13}C HSQC, ^{1}H–^{13}C HMBC, TOCSY, and DQF − COSY in ^{13}C and ^{1}H NMR. The ^{1}H–^{13}C HSQC NMR spectrum of the just prepared oxidized Dex-GMA is shown in Fig. 2A. In the figure, it can be see that $NaIO_4$ oxidizes and cleaves the C2–C3 and C3–C4 bonds in the glucose unit in dextran. In addition, the aldehyde groups react with the adjacent hydroxyl groups to form hemiacetal structures (Barman, Diehl, & Anslyn, 2014; Ouellette & Rawn, 2015). According to the NMR measurements in our previous study, oxidized dextran contains several types of hemiacetal substructure units, of which at least four substructures, including a non-oxidized glucose unit, are observed. The existence of these structures is consistent with those proposed by Ishak and Painter (1978). The four types of partial structures, including GMA immobilized oxidized dextran, and the chemical shifts of the substructures are listed in Table S1. In terms of the C2–C3 bond cleavage, oxidized glucose is converted into hemiacetal substructure 3, and the C3–C4 cleavage is consistent with hemiacetal substructure 4. Then, when the C2–C3 and C3–C4 bonds are cleaved and C3 is removed, the C2 and C4 aldehydic carbons with a water molecule are converted into hemiacetal substructure 2 (Fig. 2A bottom schemes). The DS of the GMA in oxidized Dex-GMA is calculated through 1D ^{1}H NMR (Fig. 2B). The proton chemical shift of the Dex-GMA spectrum results in new proton peaks that exhibit resonances

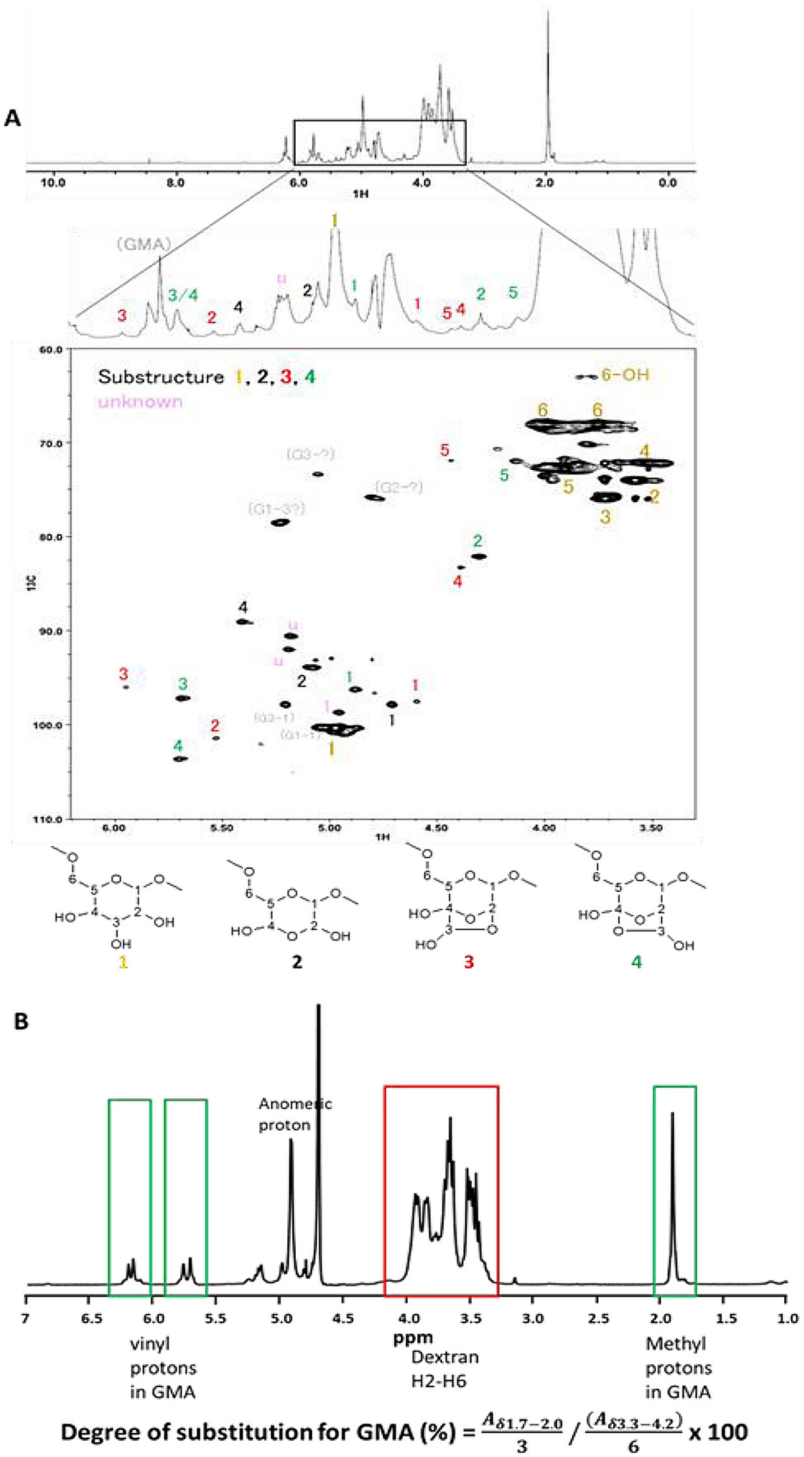

Fig. 2. NMR Spectra of oxidized Dex-GMA. (A) ^{13}C–^{1}H HSQC NMR spectrum of newly oxidized Dex-GMA. Assignments of substructures 2 (black), 3 (red), and 4 (green), non-oxidized glucose (yellow), and GMA (gray) are indicated close to the NMR signals in HSQC and 1D ^{1}H NMR. The assignment numbers represent the positions of ^{1}H and ^{13}C in each substructure. The substructures that were identified in oxidized Dex-GMA are 1: glucose, 2: C2–C3 and C3–C4 cleavage, C3 desorption, hemiacetal structure, 3: C2–C3 cleavage, hemiacetal structure, 4: C3–C4 cleavage, hemiacetal structure. (B) One-dimensional ^{1}H NMR of Dex-GMA for calculating the degree of substitution of GMA (For interpretation of the references to colour in this figure legend, the reader is referred to the web version of this article).

at 5.70–6.26 and 1.95 ppm, which are consistent with vinyl and methyl protons, respectively. The DS of the GMA in dextran is 23.1 ± 1.3%, which is calculated by comparing the ratio of the areas under the proton peaks at 2.0 ppm (methyl protons in GMA) to the peak at 3.3–4.2 ppm (dextran sugar unit protons, H2-H6) based on the NMR spectra. In Fig. S2, at least 4 types of GMA parts are observed, which might be due to different connection positions to the sugar unit, and the peaks are assigned in Table S2. The oxidized Dex-GMA spectrum should exhibit the proton chemical shift of aldehyde around 9–10 ppm. However, a peak with a low intensity at 9.6 ppm is observed instead, which is likely due to the extremely low concentration of aldehyde protons (Liu & Chan-Park, 2009; Maia et al., 2005)resulting from the abovementioned hemiacetal formation.

3.2. Determination of aldehyde content

Aldehyde content could not be quantitatively detected via the iodometric method owing to a disturbance in the reaction of the methacrylate groups in oxidized Dex-GMA and iodine (Lacroix-Desmazes, Severac, & Boutevin, 2005). Hence, aldehyde content was determined based on the reaction between AAA and formaldehyde in the presence of ammonia, which was reported by Li et al. (2007). The aldehyde content in oxidized Dex-GMA was determined using the corresponding calibration curves. The degree of oxidation was evaluated from the

oxidation percentage per glucose unit, which is defined as the number of C—C bonds cleaved in the 1,2-diol in each glucose unit. The degree of oxidation of oxidized Dex-GMA was well controlled from 10 to 41% (Fig. S3) using fluorescence intensity. This is consistent with the results presented in our previous report. In the remainder of this paper, we denote particular oxidized Dex-GMA as Ox(XX%)-GMA(YY%)-Dex, where XX is the degree of oxidation and YY is the DS of the GMA.

3.3. Gelation time of oxidized Dex-GMA with DTT

A hydrogel can be formed by mixing 10% (w/v) oxidized Dex-GMA and various concentrations of DTT in PBS at a temperature of 37 °C via a thiol Michael reaction between the methyl acrylate (from oxidized Dex-GMA) and thiol groups (from DTT) (Liu et al., 2015). An opaque white hydrogel was observed in all samples, and gelation time could be controlled by varying the molar ratio of the C=C and thiol groups (Fig. S4 A and S4B). Gelation time decreased as the amount of crosslinker DTT increased. For example, the hydrogel reached the gel point within 4.83 ± 0.53 min for a molar ratio of 1:2, which was approximately three times faster than that for a ratio of 1:0.74 (13.83 ± 0.76 min). These results indicate that gelation speed can be accelerated by increasing crosslinker concentration.

3.4. Rheological measurements

To assess the mechanical properties of the oxidized Dex-GMA based hydrogel, a rheology test (Fig. 3A and B) was performed on the hydrogels by mixing them with 1 or 1.36% DTT and 10% oxidized Dex-GMA (23% DS of GMA with varying degrees of oxidation). When 1.36% w/v of DTT was added to the 10% oxidized Dex-GMA solution, thiol and methylacrylate were present in equivalent amounts, and the thiol content was less than the amount of methylacrylate when 1% w/v of DTT was added. Higher concentrations of DTT corresponded to higher levels of G' owing to the increase in crosslinking points. The oxidized

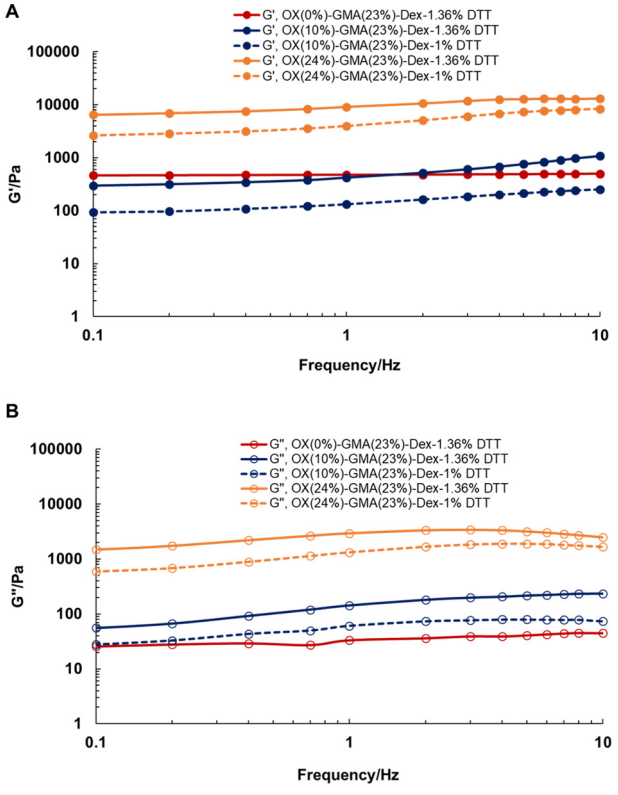

Fig. 3. Dynamic moduli of various oxidized Dex-GMA based hydrogels: (A) G' and (B) G".

Dex-GMA based hydrogel with the same degree of oxidation showed dissimilar dynamic moduli when different concentrations of DTT were used. In the presence of 1.36% w/v DTT, G' and G" were higher than those for 1% w/v DTT because the amount of thiol and the number of crosslinking points decreased, which caused a decrease in the dynamic moduli (Matsumura, Nakajima, Sugai, & Hyon, 2014). Interestingly, the degree of oxidation affected the storage moduli of various hydrogels. For example, the Ox(24%)-GMA(23%)-Dex hydrogels exhibited a higher G' value compared with the Ox(10%)-GMA(23%)-Dex hydrogels (the reasons for this are discussed in Section 3.8).

Hence, these results demonstrate that mechanical properties can be controlled by changing the degree of oxidation of Dex-GMA and the concentration of the crosslinker.

In a previous work, we reported that the dynamic moduli depended on the degree of oxidation because crosslinking occurred in the reaction between the aldehyde and amine in poly-L-lysine (Matsumura et al., 2014). However, in this report, it was found that aldehyde content is not related to crosslinking. However, the results indicated that the mechanical properties of hydrogels depended on aldehyde content. This implies that the aldehyde groups may react with the thiol groups (this is analyzed in Section 3.8). We were able to control the mechanical properties of the hydrogels from 0.1 to 10 kPa using DTT and oxidized Dex-GMA with varying degrees of oxidation.

3.5. Quantitative gel degradation

The gel formulation of oxidized Dex-GMA was produced by crosslinking oxidized Dex-GMA with DTT, which resulted in an opaque white hydrogel. In a previous study, glycine was used as a monoamine source to control the degradation of oxidized dextran (Chimpibul et al., 2016). In this study, glycine was also used to react with the remaining aldehyde in the oxidized Dex-GMA hydrogel that had been prepared via DTT crosslinking. As shown in Figs. 4A and B, the addition of glycine (an amine source) causes the gel to degrade. During the degradation process, the color of the hydrogels changed to brown after being left in a glycine solution. This indicates that a Maillard reaction occurred after a Schiff base formed between the aldehyde and primary amino groups (Chimpibul et al., 2016; Matsumura et al., 2014; Shen, Tseng, & Wu, 2007). Fig. 4A shows the gel degradation at different degrees of oxidation (0%, 10%, and 24% oxidation) and concentrations of DTT (1% and 1.36% w/v) in the presence of a glycine solution. The Ox(0%)-GMA(23%)-Dex and Ox(10%)-GMA(23%)-Dex hydrogels exhibit the same G' after reacting with 1.36% w/v DTT, as shown in Fig. 3A. Additionally, the crosslink density (ν) and degradation % 8 days after gelation are provided in Table S3. As ν is obtained from G', higher crosslink density is observed at higher G'. The differences in the hydrogel degradations are represented by the solid red and blue lines (Fig. 4A). Almost 100% of the remaining weight is observed in the Ox(0%)-GMA(23%)-Dex hydrogel but no hydrogel remains in the case of the Ox(10%)-GMA(23%)-Dex hydrogel after eight days even with the same ν. This is likely because there are no aldehyde groups in the gel to react with the amino groups from the glycine solution; thus, degradation does not occur. In addition, the hydrogels with 10% oxidation but different concentrations of the DTT crosslinker exhibit the same degradation but differing mechanical strengths and ν, as indicated by the solid and dashed blue lines. This may be because the number of crosslinking points is different at various concentrations of DTT, which has differing mechanical properties and ν; however, the number of degradation points (aldehyde groups) is the same. Therefore, the degradation pattern is the same. In the case of the Ox(24%)-GMA(23%)-Dex hydrogel, the mechanical properties are different when DTT concentrations are 1.36% and 1% (orange solid and dashed lines in Fig. 3A); however, the degradation after the addition of glycine shows a similar trend (orange solid and dashed lines in Fig. 4A). These findings clearly suggest that degradation speed can be controlled independently of the mechanical strength of the hydrogels.

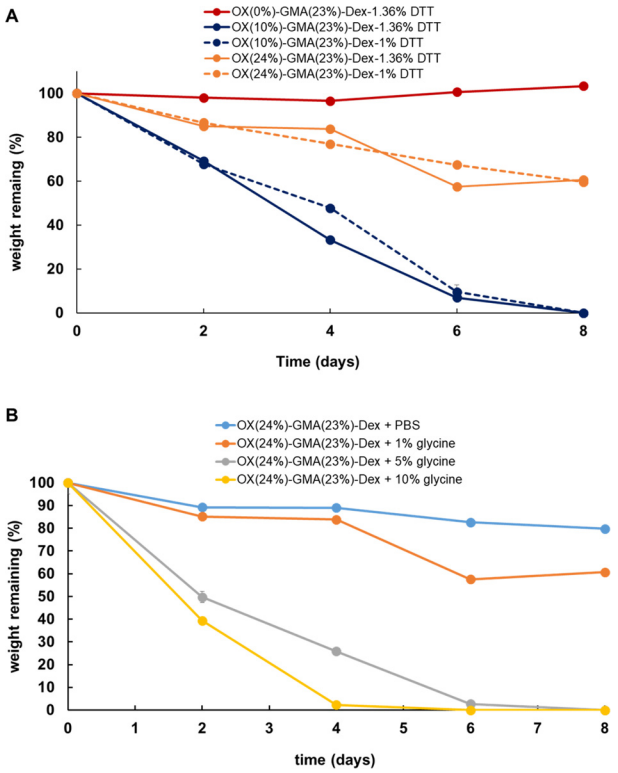

Fig. 4. Degradation of the oxidized Dex-GMA (23% DS of GMA) hydrogel at 37 °C. (A) Gel degradation at different degrees of oxidation and different concentrations of DTT in a 1% w/v glycine solution. (B) Gel degradation of oxidized Dex-GMA with 23% DS of GMA and 24% oxidation at different concentrations of glycine.

In Fig. 4B, the remaining weight of the Ox(24%)-GMA(23%)-Dex hydrogel with 1.36% DTT in 0–10% glycine PBS solutions is plotted. After eight days, more than 80% of the Ox(24%)-GMA(23%)-Dex based hydrogel remains in the PBS that does not contain glycine, and the gradual decrease that is observed may be due to the hydrolysis of ester bonds. In contrast, the degradation of the hydrogels in the presence of glycine is found to be dependent on concentration. The remaining weight of the Ox(24%)-GMA(23%)-Dex hydrogel after eight days of incubation in 1% glycine is 60.7%, while complete degradation is observed in 5% and 10% glycine solutions. In the latter cases, the majority of the degradation is observed in the first four days. This suggests that the degradation reaction is faster than the hydrolysis of ester bonds and that the degradation of the hydrogels is triggered by the reaction between the aldehyde and amino groups. The oxidized Dex-GMA based hydrogel is stable in PBS but degrades in the presence of glycine. This suggests that the degradation of the oxidized Dex-GMA hydrogel can be controlled by adding an amino source and that the rate of degradation can be accelerated by increasing the concentration of the amino source. To confirm the degradation of oxidized Dex-GMA, GPC was used to track the decrease in the molecular weight of the polymer.

3.6. Determining molecular weight via GPC

In this section, the decrease in the molecular weight of oxidized Dex-GMA after reacting with the mono-thiol reagent, Ac-Cys-OH, and glycine is described. The molecular weight of various samples after reacting with Ac-Cys-OH and glycine solutions of various concentrations were recorded through GPC, as shown in Fig. 5. As shown in the figure, when Ox(24%)-GMA(23%)-Dex (1% w/v) reacts with 0.3 and 2.5% w/v of Ac-Cys-OH (here, the thiol amount is similar and eight times higher than C = C concentration, respectively), the molecular weight remains unchanged after 3 h. The molecular weight of Ox(24%)-GMA(23%)-Dex decreases rapidly in glycine solution during the first 30 min, and then reduces gradually until it becomes steady. This is consistent with the results of the previously reported molecular degradation of oxidized dextran by glycine and suggests that GMA conjugation does not affect the degradation. In this study, we conclude that the hydrogel formed via the thiol Michael addition between the GMA and thiol is stable in the PBS. The degradation of the hydrogel is controlled by the a posteriori addition of amine sources through main chain scission via a Maillard reaction independent of the mechanical properties.

In addition, the molecular weight distributions in terms of the Mw/Mn of various oxidized Dex-GMA samples are shown in Fig. S5A. The Mw/Mn of all samples decreases in the presence of glycine solution. In literature (McCoy & Madras, 1997; Nishida et al., 2000; Sánchez-Jiménez, Pérez-Maqueda, Perejón, & Criado, 2010), random chain scission shows that molecular weight distribution should be converged to 2. However, in our case, the degradation points are aldehyde groups and these aldehyde groups have various substructures, each with different degradability (this is discussed in Section 3.8). The aldehyde groups at the degradation points are randomly introduced by oxidation. Additionally, if each oxidized part is cleaved, the length of the fragment can converge to the length of two adjacent aldehydes. Therefore, the degradation is extremely complicated, and it might be difficult to fit with currently proposed kinetic degradation models. Moreover, we show the cumulative mass distribution of Ox(24%)-GMA(23%)-Dex with glycine in Fig. S5B. It clearly seen that glycine is the main component of the mixture. Hence, it is difficult to estimate the degraded polymer structure. However, the kinetic analysis of the substructures of Ox(24%)-GMA(23%)-Dex after thiol and glycine addition was used to attain further insights into the degradation from the viewpoint of the structures. The kinetic analysis was performed using NMR, and it is discussed in Section 3.8.

The addition of thiol into Ox(24%)-GMA(23%)-Dex (green and orange lines in Fig. 5) results in almost no molecular degradation. This suggests that the thiol and GMA reaction do not affect the degradation of the polymer chain. Interestingly, slower degradation is observed when Ox(24%)-GMA(0%)-Dex is mixed with thiol (black and yellow lines in Fig. 5). This indicates that the aldehyde may react with the thiol and accelerate the molecular scission in the polymer main chain. To confirm this, the detailed reaction kinetics analyses of the reaction between the thiol and aldehyde and the thiol and GMA were performed using the 2D NMR technique described in the following section.

3.7. Determination of the reaction between the aldehyde and thiol

The aldehyde content in Ox(24%)-GMA(23%)-Dex in the presence of thiol groups was determined via a fluorometry method to investigate the reactivity between the aldehyde and thiol. The aldehyde content of each sample is summarized in Table 1. Without the monothiol reagent, the volume of the aldehyde group in Ox(24%)-GMA(23%)-Dex is 2.96×10^{-5} mole in 0.1 mL of solution. Interestingly, the amount of aldehyde shows a tendency to decrease when monothiol concentration increases. When 3% (w/v) thiol was added, the volumes of the thiol and methacrylate were equivalent in the solution. When 1.5 and 3.0% Ac-Cys-OH were added, the amount of aldehyde did not significantly decrease; however, when 5% of Ac-Cys-OH was added, the aldehyde amount decreased significantly. This suggests that the thiol groups were able to react with the aldehyde.

To confirm the reaction of the aldehyde in oxidized Dex-GMA with the thiol groups from DTT, Ox(24%)-GMA(0%)-Dex (without introducing GMA) was used as a model to react with the monothiol reagent, Ac-Cys-OH. Ellman's reagent was used to estimate the amount of sulfhydryl groups remaining in the sample. Here, a fixed amount of Ac-Cys-OH was added to the solution of oxidized dextran with various concentrations. The results showed that the concentration of the thiol groups decreased when the amount of oxidized dextran increased, as shown in

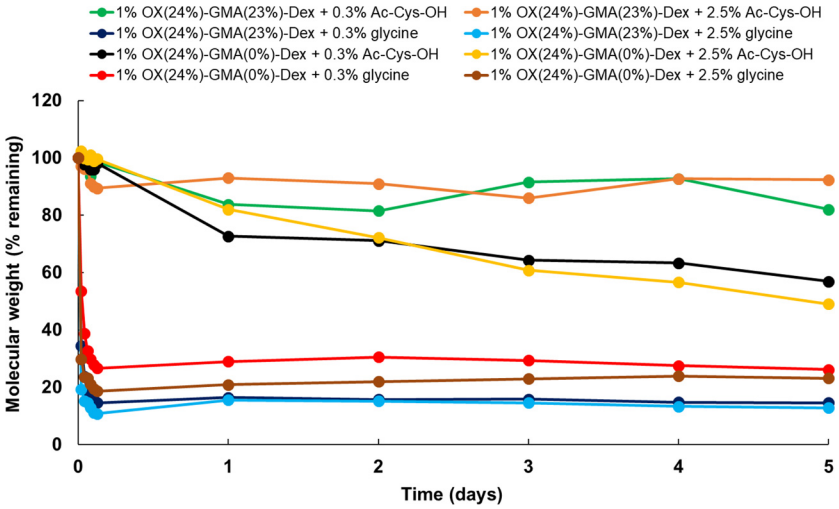

Fig. 5. Changes in the molecular weight of oxidized Dex-GMA (23% DS of GMA and 24% oxidation) and oxidized dextran (24% oxidation) in the presence of a monothiol reagent and glycine during five days.

Table 1
Analytical results for determining the aldehyde content in oxidized Dex-GMA.

Sample	-CHO found in 0.1 mL of 10% Ox(24%)-GMA(23%)-Dex ($\times 10^{-5}$ mole)
Ox(24%)-GMA(23%)-Dex + 0% (w/v) Ac-Cys-OH	2.96 ± 0.41
Ox(24%)-GMA(23%)-Dex + 1.5% (w/v) Ac-Cys-OH	2.77 ± 0.15
Ox(24%)-GMA(23%)-Dex + 3% (w/v) Ac-Cys-OH	2.55 ± 0.35
Ox(24%)-GMA(23%)-Dex + 5% (w/v) Ac-Cys-OH	1.94 ± 0.81***

Different from 0% (w/v) of Ac-Cys-OH at *** $p < 0.035$.

Fig. S6. Based on this, it can be concluded that the aldehyde can react with the thiol groups. According to literature, thiol reacts with aldehydes to produce hemithioacetal (Fife & Anderson, 1970; Sakulsombat, Zhang, & Ramstrom, 2012). However, from the result of Table 1, the thiol group reacts dominantly with the methacrylate group via a thiol Michael addition reaction. Thus, less DTT should be added compared to immobilized GMA in oxidized Dex-GMA to preserve the aldehyde groups after gel formation. The proposed model describing the formation of an oxidized Dex-GMA based hydrogel is shown in Fig. 1B. The remaining aldehyde reacts with the amine sources after gel formation; this results in the degradation reaction (Fig. 1C).

3.8. Kinetic analysis of the reaction between the GMA and thiol and the aldehyde and thiol by NMR

The identified time-dependent NMR peak changes in 5% Ox(24%)-GMA(23%)-Dex with 0.75% Ac-Cys-OH (low concentration condition) are shown in Fig. 6. Under these conditions, there is more C=C compared to thiol. Fig. 6A shows the time-dependent peak intensity changes via the red and blue lines. The kinetics of the specific peaks are shown in Figs. 6B–F. The aldehyde groups in the oxidized part react with adjacent hydroxyl groups to form hemiacetal substructures (substructures 2–4). The proton peaks in substructures 2 and 4 and Ac-Cys-OH decrease (Figs. 6B, C, and F). In contrast, the peaks of the GMA vinyl protons and substructure 3 show no decrease in intensity (Figs. 6D and E). This suggests that the thiol reacts quickly with aldehyde substructures 2 and 4, and not with the vinyl protons in GMA. Substructure 3 does not react with the thiol under these conditions. The time-dependent NMR peak changes in 5% Ox(24%)-GMA(23%)-Dex with 3% Ac-Cys-OH (high concentration condition) are shown in Fig. 7. Under these conditions, there is more thiol compared to C=C. The peak intensity of the vinyl protons in GMA (5.8 and 6.2 ppm) decreases rapidly after the reaction with the thiol groups (Fig. 7B) after a time constant of 0.53 h.

Under these conditions, the protons from all substructures decrease after mixing with the thiol. Substructures 2 (H4 peak at 5.40 ppm) and 4 (H3/4 peak at 5.72 ppm) exhibit extremely rapid decomposition, which implies that the reaction is almost finished by the time the measurement starts. However, substructure 3 (Fig. 7C, H2 peak at 5.53 ppm) decomposes with a time constant of 4.33 h, which is slower than the time for the GMA peak to diminish, which had a time constant of 0.53 h. Comparing the speed of reaction with the thiol, it can be said that substructures 2 and 4 are faster than GMA and substructure 3 is slower than GMA.

The reaction products of the thiol and aldehyde are shown in Figs. 8 and S7. These peaks are assigned to monothioacetal protons. Under high concentrations of the thiol, the proton peaks of the reaction products are so broad that they cannot be assigned to the structures. At low concentrations, the thioacetal production can be allocated between the thiol and substructure 4 by HSQC and HMBC (Fig. S7A). In low concentration Ac-Cys-OH conditions, most of the thiol is consumed to produce thioacetal with aldehydes, which suggests fast reaction aldehydes. This can be confirmed by the increase in the thiocetal proton peak (Fig. S8). Based on this, it is determined that the aldehyde (substructure 4), which reacts quickly with the thiol, forms thioacetal, based on which the main structure of the product is assigned (Fig. 8). By comparing the production peaks between low and high concentrations of Ac-Cys-OH, we detect the same proton peaks in the high concentration condition, which indicates that thioacetal is produced even in high Ac-Cys-OH conditions (Fig. S7B). It is determined that stable thioacetal (Kyprianou et al., 2010) also contributes to the crosslinks in addition to the thiol-ene crosslinking during hydrogel formation by oxidized Dex-GMA and DTT. This is why the storage moduli in the Ox(24%)-GMA(23%)-Dex hydrogel are higher than those in the Ox(0%)-GMA(23%)-Dex or Ox(10%)-GMA(23%)-Dex hydrogels (Fig. 3A). This is also supported by the observation that oxidized dextran without GMA takes the form of a hydrogel when mixed with DTT. However, gelation time is extremely slow, which suggests that the crosslinking by thioacetal may not be dominant. As shown in Fig. S9, we detect a reduction in end proton production only in high concentration Ac-Cys-OH

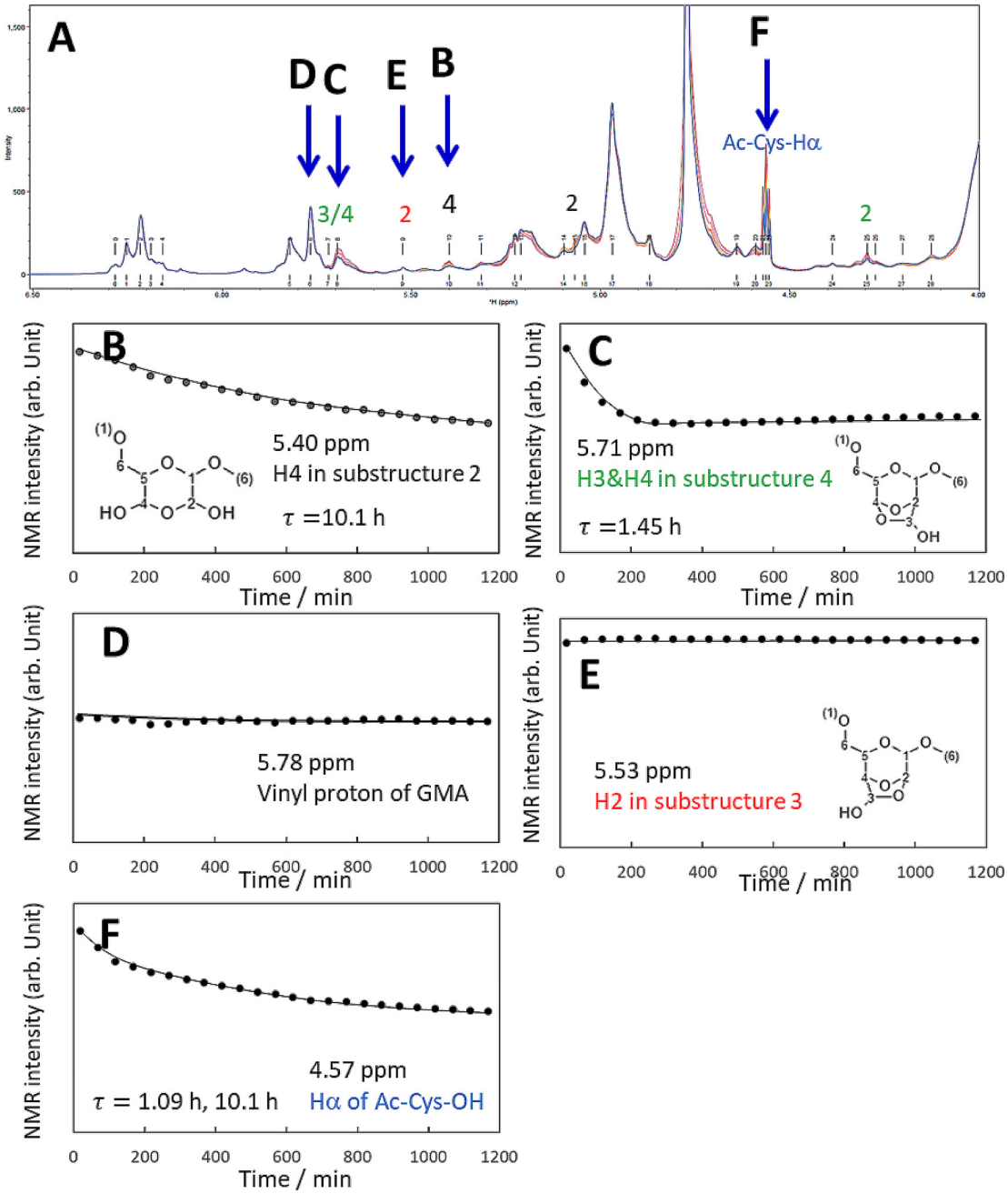

Fig. 6. (A) One-dimensional ^{1}H NMR spectra of the reaction of 5% Ox(24%)-GMA(23%)-Dex and 0.75% Ac-Cys-OH (low concentration condition), and kinetic analysis of the time-course NMR spectra for (B) substructure 2, (C) substructure 4, (D) vinyl group, (E) substructure 3, and (F) α proton of Ac-Cys-OH. The solid lines are computed by single-exponential curve fitting, and the time constants (τ) of the exponential function are shown.

conditions (black dots surrounded by circles). More rapid reductions in the number of end protons in the glucose unit are considered as the evidence of main chain scission. This result suggests that the molecular degradation in the polysaccharide main chain also occurs after the reaction between the thiol and slow reacting aldehyde, which contradicts the GPC results. However, in Fig. 5B, the yellow and black lines (Ox (24%)-GMA(0%)-Dex and thiol reaction) indicate gradual degradation, which may be the result of main chain scission after the aldehyde and thiol reaction. However, a more detailed quantitative analysis is required to confirm this. Furthermore, in Fig. 4B, the Ox(24%)-GMA(23%)-Dex hydrogel exhibits slight degradation in PBS without an amine source, which be due to not only ester hydrolysis but also the main chain degradation caused by the thiol and aldehyde reaction. However, there are multiple crosslinking points of thiol-ene and thiol-aldehyde, which should have delayed the degradation of the hydrogel. The rapid aldehyde reaction (substructure 2, 4) forms thioacetal with SH, followed by the reaction of SH with GMA. Then, as SH reacts with substructure 3 and generates reducing ends, this suggests that it is involved in molecular decomposition.

In Fig. S10, we confirm the rapid decomposition of the aldehydes (hemiacetal substructure 2) in the Ox(24%)-GMA(23%)-Dex and glycine (model of amine source) mixture. In addition, the reduction in the end proton signal suggests that main chain scission increases. Interestingly, based on the peaks shown in Fig. S11 around 2.2 ppm, methylene groups are generated. This is ascribed to 3-deoxyosone during the progress of the Maillard reaction (Fig. S1), which is consistent with a previous report (Chimpibul et al., 2016), including the introduction of GMA. However, these methylene proton peaks are not

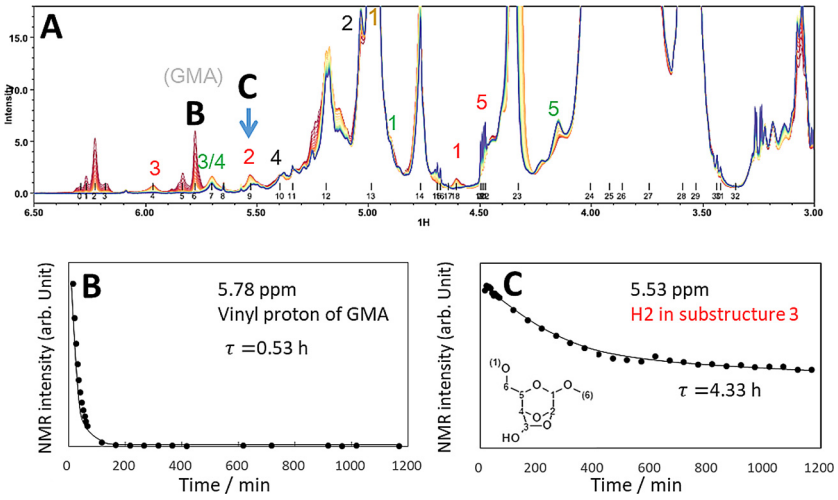

Fig. 7. (A) One-dimensional ^{1}H NMR spectra of reaction of 5% Ox(24%)-GMA(23%)-Dex and 3% Ac-Cys-OH (high concentration condition), and kinetic analysis of the time-course NMR spectra for (B) the vinyl group and (C) substructure 3. Solid lines are calculated by single-exponential curve fitting, and the time constants (τ) of the exponential function are shown.

observed in the mixture of Ox(24%)-GMA(23%)-Dex and Ac-Cys-OH, which suggests there is a different degradation pathway between the aldehyde and thiol and aldehyde and amine reactions. This is also confirmed by the change in the color of the hydrogels; for example, the addition of glycine causes the hydrogels to turn brown. Therefore, we conclude that the reaction mechanism is as follows: There are fast and slow reactive aldehyde substructures in oxidized Dex-GMA, and the fast reactive substructures react with the thiol to produce thioacetal, which results in crosslinking. Then, the thiol reacts with GMA to produce dominant crosslinking points, followed by the slow reactive aldehydes reacting with the thiol and contributing to the main chain scission of oxidized Dex-GMA. Finally, the a posteriori addition of amine results in a reaction with hemiacetal, which leads to a Maillard reaction via dexyosone production and accelerates the degradation. Considering these complicated reaction mechanisms, we were able to prepare hydrogels in which degradation timing was controlled independently of mechanical properties.

3.9. Cytotoxicity assay

The cytotoxicity of dextran, Ox-(24%)-GMA(23%)-Dex, and glutaraldehyde to L929 cells was evaluated through MTT assay, and the results are provided in Fig. S12 and Table S4. The IC50 of Ox(24%)-GMA(23%)-Dex is 15362 ± 1353 μg/mL (1.5 w/w %), demonstrating lower cytotoxicity than glutaraldehyde (IC50 is 5.6 μg/mL). Even though the cytotoxicity of aldehyde dextran is enhanced by the oxidation and introduction of aldehyde, the cytotoxicity is still 1/3000 that of glutaraldehyde. Such low toxicity of oxidized dextran is consistent with our previous report (Hyon et al., 2014). The low cytotoxicity of aldehyde in the oxidized dextran is likely caused by its low reactivity (Hyon et al., 2014) with amine species due to the hemiacetal formation described in a later section.

4. Conclusion

We introduced GMA into oxidized dextran and formed a hydrogel with DTT while preserving the aldehyde to overcome the major drawback of oxidized dextran and polyamine hydrogels, i.e., uncontrollable degradation. In our proposed formulation, degradation did not occur immediately after the hydrogels were formed. Instead, degradation could be controlled by the a posteriori addition of an amine source, and interestingly, degradation speed could be controlled independently of the mechanical properties of the hydrogel. The mechanical properties depended on the number of crosslinking points, and NMR was used to determine that the GMA and aldehyde groups reacted with the thiol to form crosslinking points. Thus, the mechanical properties could be controlled by the numbers of the GMA–thiol and aldehyde–thiol crosslinks. The addition of amine began a reaction with the remaining aldehyde, which triggered degradation through a Maillard reaction via a Schiff base reaction. To the best of our knowledge, this is the first time that the details of these degradation mechanisms have been elucidated at the molecular level. This level of understanding of the mechanism of molecular degradation is an important step toward the design of polymer materials in which degradation can be precisely controlled. In

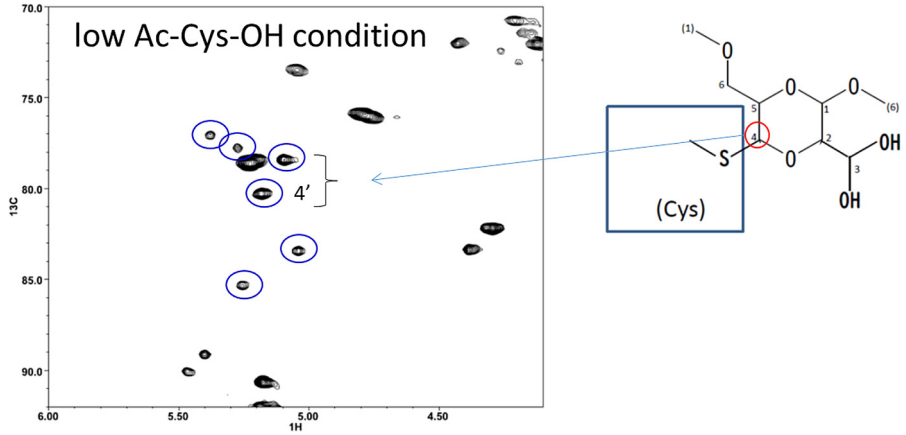

Fig. 8. ^{13}C-^{1}H HSQC NMR spectrum of 5% Ox(24%)-GMA(23%)-Dex and 0.75% Ac-Cys-OH and the estimated main structure of the thioacetal produced by the reaction between thiol and aldehyde (substructure 4).

the human body, there are several amine sources, such as proteins. Therefore, our hydrogel must be capable of biodegradation. Furthermore, to definitively demonstrate degradation control, we plan to conduct a long-term study involving a few combinations of stimuli (temperature) responsive hydrogels that incorporate amine sources to release amine and start degradation. If successful, these hydrogels with finely tunable stimuli responsive degradations could open new avenues not only in biomedical and tissue engineering fields but also in agriculture or environmental fields, such as in external stimuli responsive drug delivery applications.

Conflict of interest

The authors declare no competing financial interest.

Appendix A. Supplementary data

Supplementary material related to this article can be found, in the online version, at doi:https://doi.org/10.1016/j.carbpol.2018.09.081.

References

Augst, A. D., Kong, H. J., & Mooney, D. J. (2006). Alginate hydrogels as biomaterials. *Macromolecular Bioscience, 6*(8), 623–633.

Barman, S., Diehl, K. L., & Anslyn, E. V. (2014). The effect of alkylation, protonation, and hydroxyl group substitution on reversible alcohol and water addition to 2- and 4-formyl pyridine derivatives. *RSC Advances, 4*(55), 28893–28900.

Bhattarai, N., Gunn, J., & Zhang, M. (2010). Chitosan-based hydrogels for controlled, localized drug delivery. *Advanced Drug Delivery Reviews, 62*(1), 83–99.

Bouhadir, K. H., Lee, K. Y., Alsberg, E., Damm, K. L., Anderson, K. W., & Mooney, D. J. (2001). Degradation of partially oxidized alginate and its potential application for tissue engineering. *Biotechnology Progress, 17*(5), 945–950.

Cadee, J. A., van Luyn, M. J., Brouwer, L. A., Plantinga, J. A., van Wachem, P. B., de Groot, C. J., et al. (2000). In vivo biocompatibility of dextran-based hydrogels. *Journal of Biomedical Materials Research, 50*(3), 397–404.

Chen, Y. M., Sun, L., Yang, S. A., Shi, L., Zheng, W. J., Wei, Z., et al. (2017). Self-healing and photoluminescent carboxymethyl cellulose-based hydrogels. *European Polymer Journal, 94*, 501–551.

Chimpibul, W., Nagashima, T., Hayashi, F., Nakajima, N., Hyon, S. H., & Matsumura, K. (2016). Dextran oxidized by a malaprade reaction shows main chain scission through a maillard reaction triggered by schiff base formation between aldehydes and amines. *Journal of Polymer Science Part A, 54*(14), 2254–2260.

Debele, T. A., Mekuria, S. L., & Tsai, H. C. (2016). Polysaccharide based nanogels in the drug delivery system: Application as the carrier of pharmaceutical agents. *Materials Science and Engineering C, 68*, 964–981.

Ferreira, L., Rafael, A., Lamghari, M., Barbosa, M. A., Gil, M. H., Cabrita, A. M., et al. (2004). Biocompatibility of chemoenzymatically derived dextran-acrylate hydrogels. *Journal of Biomedical Materials Research Part A, 68*(3), 584–596.

Ferreira, L. S., Gerecht, S., Fuller, J., Shieh, H. F., Vunjak-Novakovic, G., & Langer, R. (2007). Bioactive hydrogel scaffolds for controllable vascular differentiation of human embryonic stem cells. *Biomaterials, 28*(17), 2706–2717.

Fife, T. H., & Anderson, E. (1970). Thioacetal hydrolysis. Hydrolysis of benzaldehyde methyl S-(substituted phenyl) thioacetals. *Journal of the American Chemical Society, 92*(18), 5464–5468.

Hoare, T. R., & Kohane, D. S. (2008). Hydrogels in drug delivery: Progress and challenges. *Polymer, 49*(8), 1993–2007.

Hyon, S.-H., Nakajima, N., Sugai, H., & Matsumura, K. (2014). Low cytotoxic tissue adhesive based on oxidized dextran and epsilon-poly-l-lysine. *Journal of Biomedical Materials Research Part A, 102*(8), 2511–2520.

Ishak, M. F., & Painter, T. J. (1978). Kinetic evidence for hemiacetal formation during the oxidation of dextran in aqueous periodate. *Carbohydrate Research, 64*, 189–197.

Jogani, V., Jinturkar, K., Vyas, T., & Misra, A. (2008). Recent patents review on intranasal administration for CNS drug delivery. *Recent Patents on Drug Delivery & Formulation, 2*(1), 25–40.

Jukes, J. M., van der Aa, L. J., Hiemstra, C., van Veen, T., Dijkstra, P. J., Zhong, Z., et al. (2010). A newly developed chemically crosslinked dextran-poly(ethylene glycol) hydrogel for cartilage tissue engineering. *Tissue Engineering Part A, 16*(2), 565–573.

Khalikova, E., Susi, P., & Korpela, T. (2005). Microbial dextran-hydrolyzing enzymes: Fundamentals and applications. *Microbiology and Molecular Biology Reviews, 69*(2), 306–325.

Kirchhof, S., Strasser, A., Wittmann, H. J., Messmann, V., Hammer, N., Goepferich, A. M., et al. (2015). New insights into the cross-linking and degradation mechanism of Diels-Alder hydrogels. *Journal of Materials Chemistry B, 3*(3), 449–457.

Kyprianou, D., Guerreiro, A. R., Nirschl, M., Chianella, I., Subrahmanyam, S., Turner, A. P. F., et al. (2010). The application of polythiol molecules for protein immobilisation on sensor surfaces. *Biosensors & Bioelectronics, 25*(5), 1049–1055.

Lacroix-Desmazes, P., Severac, R., & Boutevin, B. (2005). Reverse iodine transfer polymerization of methyl acrylate and n-Butyl acrylate. *Macromolecules, 38*(15), 6299–6309.

Levesque, S. G., & Shoichet, M. S. (2007). Synthesis of enzyme-degradable, peptide-cross-linked dextran hydrogels. *Bioconjugate Chemistry, 18*(3), 874–885.

Li, Q., Sritharathikhun, P., & Motomizu, S. (2007). Development of novel reagent for Hantzsch reaction for the determination of formaldehyde by spectrophotometry and fluorometry. *Analytical Sciences, 23*(4), 413–417.

Liu, Y., & Chan-Park, M. B. (2009). Hydrogel based on interpenetrating polymer networks of dextran and gelatin for vascular tissue engineering. *Biomaterials, 30*(2), 196–207.

Liu, Z., Jiao, Y., Wang, Y., Zhou, C., & Zhang, Z. (2008). Polysaccharides-based nanoparticles as drug delivery systems. *Advanced Drug Delivery Reviews, 60*(15), 1650–1662.

Liu, Z. Q., Wei, Z., Zhu, X. L., Huang, G. Y., Xu, F., Yang, J. H., et al. (2015). Dextran-based hydrogel formed by thiol-Michael addition reaction for 3D cell encapsulation. *Colloids and Surfaces B, Biointerfaces, 128*, 140–148.

Maia, J., Ferreira, L., Carvalho, R., Ramos, M. A., & Gil, M. H. (2005). Synthesis and characterization of new injectable and degradable dextran-based hydrogels. *Polymer, 46*(23), 9604–9614.

Massia, S. P., & Stark, J. (2001). Immobilized RGD peptides on surface-grafted dextran promote biospecific cell attachment. *Journal of Biomedical Materials Research, 56*(3), 390–399.

Matsumura, K., Nakajima, N., Sugai, H., & Hyon, S. H. (2014). Self-degradation of tissue adhesive based on oxidized dextran and poly-L-lysine. *Carbohydrate Polymers, 113*, 32–38.

McCoy, B. J., & Madras, G. (1997). Degradation kinetics of polymers in solution: Dynamics of molecular weight distributions. *AIChE Journal, 43*(3), 802–810.

Mehvar, R. (2000). Dextrans for targeted and sustained delivery of therapeutic and imaging agents. *Journal of Controlled Release, 69*(1), 1–25.

Möller, S., Weisser, J., Bischoff, S., & Schnabelrauch, M. (2007). Dextran and hyaluronan methacrylate based hydrogels as matrices for soft tissue reconstruction. *Biomolecular Engineering, 24*(5), 496–504.

Morris, G., Kok, S., Harding, S., & Adams, G. (2010). Polysaccharide drug delivery systems based on pectin and chitosan. *Biotechnology & Genetic Engineering Reviews, 27*, 257–284.

Nishida, H., Yamashita, M., Nagashima, M., Hattori, N., Endo, T., & Tokiwa, Y. (2000). Theoretical prediction of molecular weight on autocatalytic random hydrolysis of aliphatic polyesters. *Macromolecules, 33*(17), 6595–6601.

Ouellette, R. J., & Rawn, J. D. (2015). *19 - Aldehydes and ketones: Nucleophilic addition reactions. Organic chemistry study guide*. Boston: Elsevier335–360.

Reis, A. V., Fajardo, A. R., Schuquel, I. T. A., Guilherme, M. R., Vidotti, G. J., Rubira, A. F., et al. (2009). Reaction of Glycidyl Methacrylate at the Hydroxyl and Carboxylic Groups of Poly(vinyl alcohol) and Poly(acrylic acid): Is This Reaction Mechanism Still Unclear? *The Journal of Organic Chemistry, 74*(10), 3750–3757.

Sakulsombat, M., Zhang, Y., & Ramstrom, O. (2012). Dynamic asymmetric hemithioacetal transformation by lipase-catalyzed gamma-lactonization: In situ tandem formation of 1,3-oxathiolan-5-one derivatives. *Chemistry, 18*(20), 6129–6132.

Sánchez-Jiménez, P. E., Pérez-Maqueda, L. A., Perejón, A., & Criado, J. M. (2010). A new model for the kinetic analysis of thermal degradation of polymers driven by random scission. *Polymer Degradation and Stability, 95*(5), 733–739.

Shen, S.-C., Tseng, K. C., & Wu, J. S. B. (2007). An analysis of Maillard reaction products in ethanolic glucose–glycine solution. *Food Chemistry, 102*(1), 281–287.

Togo, Y., Takahashi, K., Saito, K., Kiso, H., Huang, B., Tsukamoto, H., et al. (2013). Aldehyded dextran and ε-Poly(L-lysine) hydrogel as nonviral gene carrier. *Stem Cells International, 2013*, 1–5.

Van Dijk-Wolthuis, W. N. E., Franssen, O., Talsma, H., van Steenbergen, M. J., Kettenes-van den Bosch, J. J., & Hennink, W. E. (1995). Synthesis, characterization, and polymerization of Glycidyl Methacrylate derivatized dextran. *Macromolecules, 28*(18), 6317–6322.

Van Tomme, S. R., & Hennink, W. E. (2007). Biodegradable dextran hydrogels for protein delivery applications. *Expert Review of Medical Devices, 4*(2), 147–164.

Zhao, W., Hai, Y. J., Qi, L. Z., Feng, X., Xiong, Z. J., Miklós, Z., et al. (2015). Novel biocompatible polysaccharide-based self-healing hydrogel. *Advanced Functional Materials, 25*(9), 1352–1359.